

# FIRST VERIFICATION OF SCIAMACHY'S ABSORBING AEROSOL INDEX PRODUCT

M. de Graaf and P. Stammes

*Royal Netherlands Meteorological Institute (KNMI),  
P.O. Box 201, 3730 AE de Bilt, The Netherlands  
Email: graafdem@knmi.nl, stammes@knmi.nl*

## ABSTRACT

Some preliminary results about the verification and validation of SCIAMACHY's Absorbing Aerosol Index (AAI) are presented. The operational AAI level 2 product of SCIAMACHY is compared to our own AAI algorithm, developed at KNMI. The operational product shows general agreement with the KNMI algorithm but both suffer from large errors in reflectances, resulting in a large off-set. Also, the neglect of polarisation in the operational product introduces significant errors.

## 1. INTRODUCTION

The Absorbing Aerosol Index (AAI) is a measure for the presence of dark (i.e. absorbing) aerosols in the Earth's atmosphere. It is an operational (near-real time) SCIAMACHY level 2 product. It uses the Earth's reflectance at two wavelengths, which is determined by the Earth's radiance, the solar irradiance, and the solar zenith angle. These are all SCIAMACHY level 1 products and as such the AAI can be used for verification of these level 1 products as well.

The AAI is defined as

$$\text{AAI} = -100 \cdot \left\{ {}^{10}\log\left(\frac{I_\lambda}{I_{\lambda_0}}\right)_{meas} - {}^{10}\log\left(\frac{I_\lambda}{I_{\lambda_0}}\right)_{Ray} \right\}, \quad (1)$$

where  $I_\lambda$  is the radiance at the top of the atmosphere (TOA) at a wavelength  $\lambda$ . The subscript *meas* refers to a measured real atmosphere TOA radiance, as opposed to a TOA radiance in a Rayleigh atmosphere, where only (multiple) scattering from gases and surface reflection occurs. The latter is referred to as *Ray*. The reflectance is defined as

$$R = \frac{\pi I}{\mu_0 E_0}, \quad (2)$$

where  $E_0$  is the solar irradiance at TOA perpendicular to the direction of the incident sunlight and  $\mu_0$  is the cosine of the solar zenith angle  $\theta_0$ . So  $\mu_0 E_0$  is the solar irradiance at TOA incident on a horizontal surface unit.

If the surface albedo for the Rayleigh atmosphere calculation is chosen so that  $(I_{\lambda_0})_{meas} = (I_{\lambda_0})_{Ray}$ , where  $\lambda_0$  is some reference wavelength, then equation (1) can be reduced to

$$\text{AAI} = -100 \cdot {}^{10}\log\left(\frac{(R_\lambda)_{meas}}{(R_\lambda)_{Ray}}\right), \quad (3)$$

where  $(R_\lambda)_{Ray}$  is dependent on the surface albedo. The radiances in equation (1) are replaced by reflectances, because according to equation (2) quotients of radiances are equal to quotients of reflectances.

As has been shown before [1] the AAI is dependent on the amount of absorbing aerosols in the atmosphere, on the altitude of the aerosol layer in the atmosphere, on the presence of clouds, as well as on the ground pressure and the presence of absorbing gases, particularly ozone.

## 2. COMPUTATIONAL METHOD OF THE OPERATIONAL AAI

The reflectance in a Rayleigh atmosphere can be calculated with a radiative transfer code. For the SCIAMACHY operational processor a Look-Up Table (LUT) was created relating reflectance to surface albedo. To parameterize the geometry, polynomial fitting was used for the solar zenith angle (6 coefficients) and the viewing zenith angle dependence (3 coefficients), while the azimuth dependence in a Rayleigh atmosphere can be represented by a Fourier series of only three terms. So 72 coefficients are used to represent the geometry. To correct for the surface pressure, 11 reference heights, from 0 to 5 km (resolution 0.5 km) are represented in the LUT. The SCIAMACHY AAI can be calculated for 15 reference wavelengths  $\lambda_0$ , between 340 and 410 nm (resolution 5 nm). From now on we will always take 380 nm as the reference wavelength  $\lambda_0$  and 340 nm as  $\lambda$ . No correction

can be made for the presence of ozone or other absorbing gases. The computational method of the operational AAI is described in more detail in [2].

### 3. COMPUTATIONAL METHOD OF THE KNMI AAI ALGORITHM

The code used to generate the LUTs of the operational processor neglects polarisation and it can be shown [1] that this will generate AAI errors up to 4, which is in the order of the maximum AAI expected. To correct for this, a new algorithm for the AAI was written at KNMI and new Rayleigh LUTs were created using the Doubling-Adding KNMI (DAK) radiative transfer code in which polarisation can be accounted for. The effect of polarisation in DAK is described in detail by Stammes [3].

In the new LUTs cubic spline interpolation over 42 non-equidistant points in the solar zenith and viewing zenith angles direction is used to get three Fourier coefficients for the azimuth dependence. Tables can be created for every wavelength pair desired. A second order interpolation is made in the reference height, where values are given at 0 km (1013 hPa), 2 km and 5 km. Also, to account for ozone, a linear interpolation is performed between 1 and 1.5 times the standard ozone column (334 DU) or 1 and 0.5 times the standard ozone column.

The new algorithm has been compared to the operational level 2 AAI product of SCIAMACHY.

### 4. RESULTS FOR THE OPERATIONAL AAI

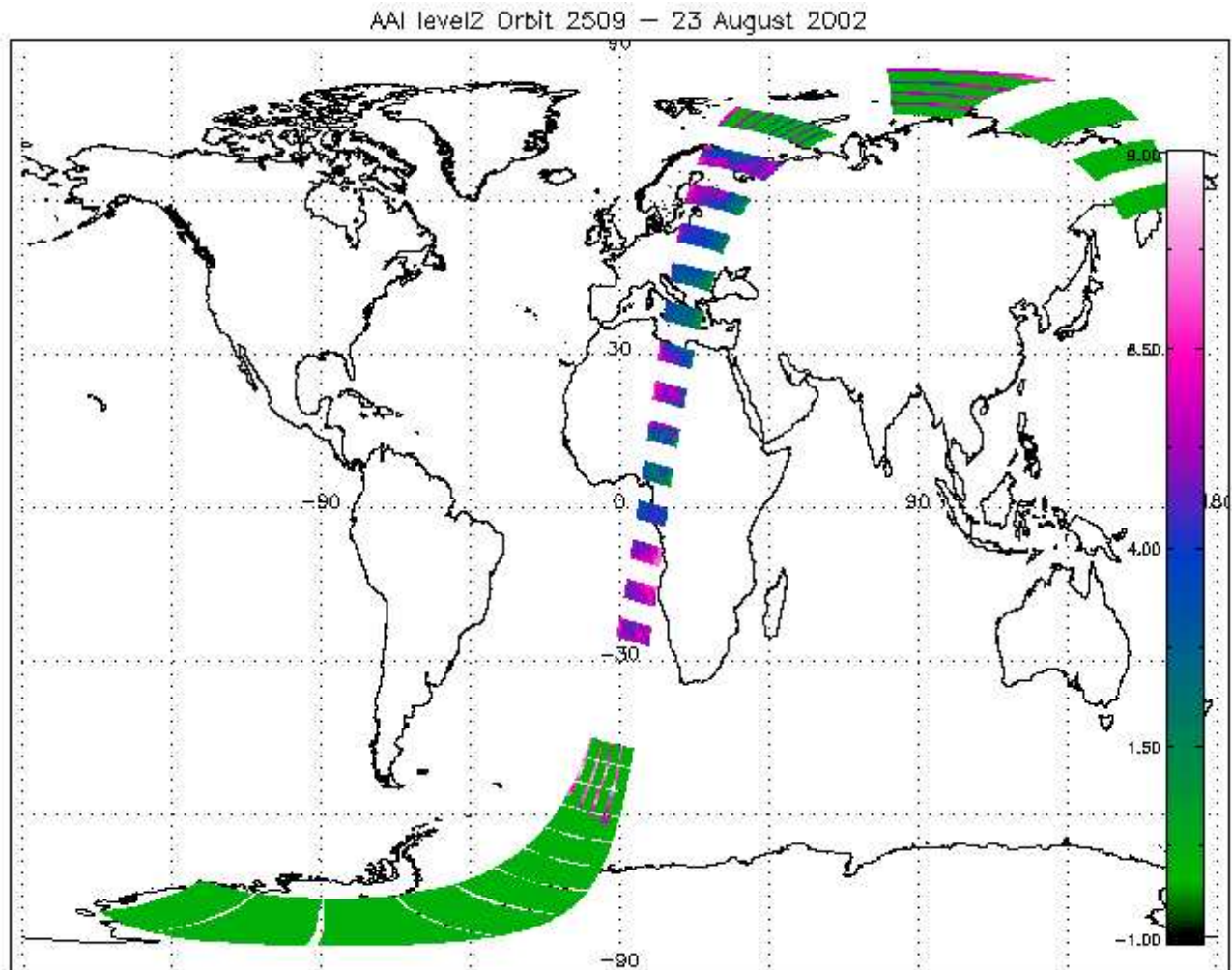


Fig. 1: AAI level 2, orbit 2509 on 23 August 2002

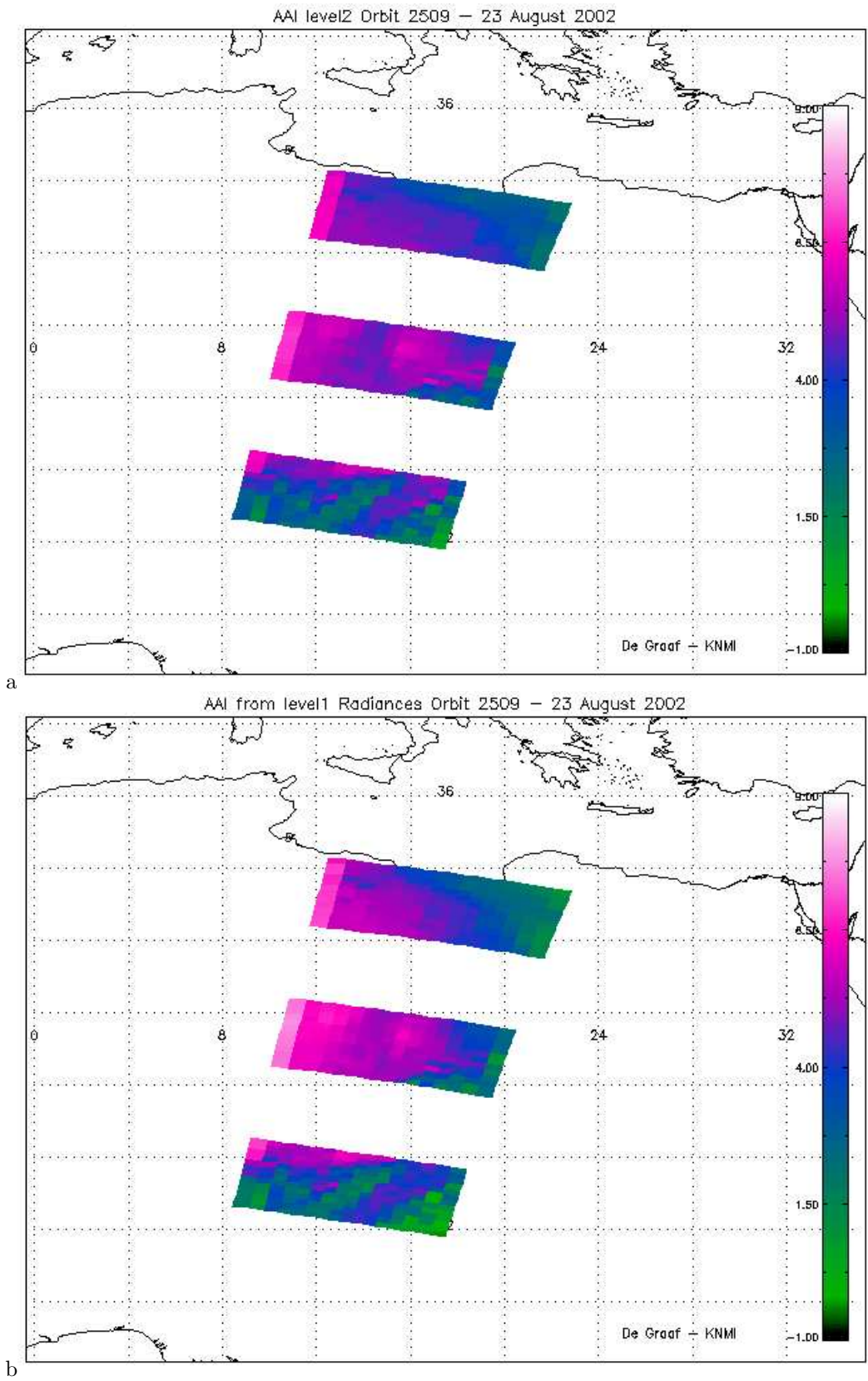


Fig. 2: AAI, orbit 2509 on 23 August 2002. Top panel shows SCIAMACHY's level 2 product, a close-up of fig. 1 over the Sahara with states 11-13, bottom panel shows the AAI derived from SCIAMACHY level 1 radiances.

In fig. 1 the operational AAI level 2 product of SCIAMACHY is given for orbit 2509. This is an orbit of 23 August 2002 over Europe and northern Africa, which was reprocessed by the updated processor of November 2002 (version 4.00). We will concentrate on three states over the Sahara in Africa. These states (11-13) are shown in more detail in fig. 2a.

The operational AAI in these three states shows that the amplitude is in the order that is expected, but it has an off-set. The maximum AAIs expected are about -4 to 4, while the level 2 product varies between -1 and 9. It has high values over the entire orbit, while it is expected to find only slightly positive values in selected regions containing elevated absorbing aerosols. It shows physical structures, except for a light band at the extreme west pixels.

## 5. RESULTS FOR THE KNMI AAI ALGORITHM

Fig.2b shows the AAI developed at KNMI. Comparing it with fig.2a we see that in general the pictures correspond very well. The figures have the exact same color scale and we see that the AAI values in both pictures have almost the same values. The KNMI AAI seems to have a slightly higher amplitude. This is confirmed in fig. 3, where both AAIs are plotted as a function of pixel index for the middle of the three states, i.e. state 12. The structures in both the operational level 2 AAI and the KNMI AAI are the same, although in the KNMI AAI they are more pronounced, because of the larger amplitude.

## 6. DISCUSSION OF THE DIFFERENCES

The KNMI AAI has approximately the same scale as the operational level 2 product, between -1 and 9, apart

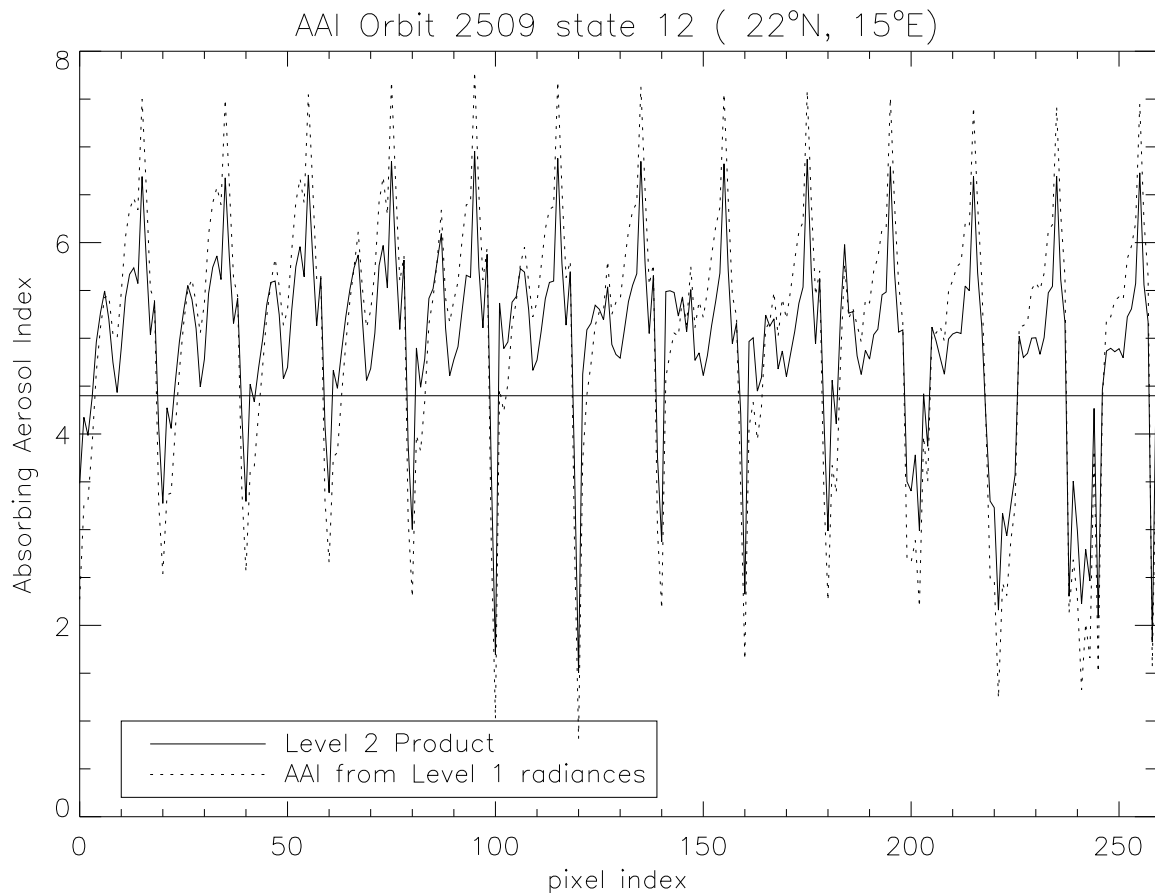


Fig. 3: AAI in state 12 of orbit 2509, 23 August 2002 as a function of pixel index. Solid line is the SCIAMACHY operational level 2 AAI product, dotted line is the KNMI AAI.

from a slightly larger amplitude. This is much higher than the expected range, which is about -4 to 4. This suggests an off-set error. At the SCIAMACHY workshop of November 2002, R. Siddans (RAL) reported that the level 1 reflectance of SCIAMACHY was about 20% lower than expected from validation measurements. Using this amount in a theoretical study an off-set of 4.4 in the AAI was found. In fig. 4 this is explained: it shows the expected reflectances at TOA in a Rayleigh atmosphere for a certain geometry and surface reflection and the same curve with a 20% reduction. In a molecular atmosphere the reflectance shows a strong,  $\lambda^{-4}$ , wavelength dependence, approximately. Therefore, a reduction of 20% in reflectance will mean a much higher absolute reduction at 340 nm than at 380 nm. In other words, the slope of the reflectance at these two wavelengths is reduced, which is exactly what is measured by the AAI. In the case shown, with a Rayleigh atmosphere, a surface albedo of 5%, nadir view and a solar zenith angle of  $30^\circ$ , an AAI of 4.4 was found. As depicted in fig. 3, correcting for this off-set would bring the AAI in better agreement with the expected range.

The cloud dependence of the AAI seems correct, as follows from fig. 5. This shows the color composite of three PMD channels (2-4) of the same region over the Sahara. PMD channels are read out more frequently than the spectral channels of SCIAMACHY and thus provide higher spatial resolution images. Channels 2-4 are centered around 487 nm (blue), 661 nm (red) and 853 nm (IR) respectively. Using the last one as a green signal, a picture is obtained which shows dark oceans, green vegetation, light yellow deserts and white clouds [4]. Comparing fig. 5 with fig. 2 we see that clouds have a reducing effect on the AAI, as expected. This is especially clear in state 13, where the lowest AAI levels correspond very well with the cloudy white areas in the PMD picture. This is true for both the operational level 2 product as for the KNMI AAI.

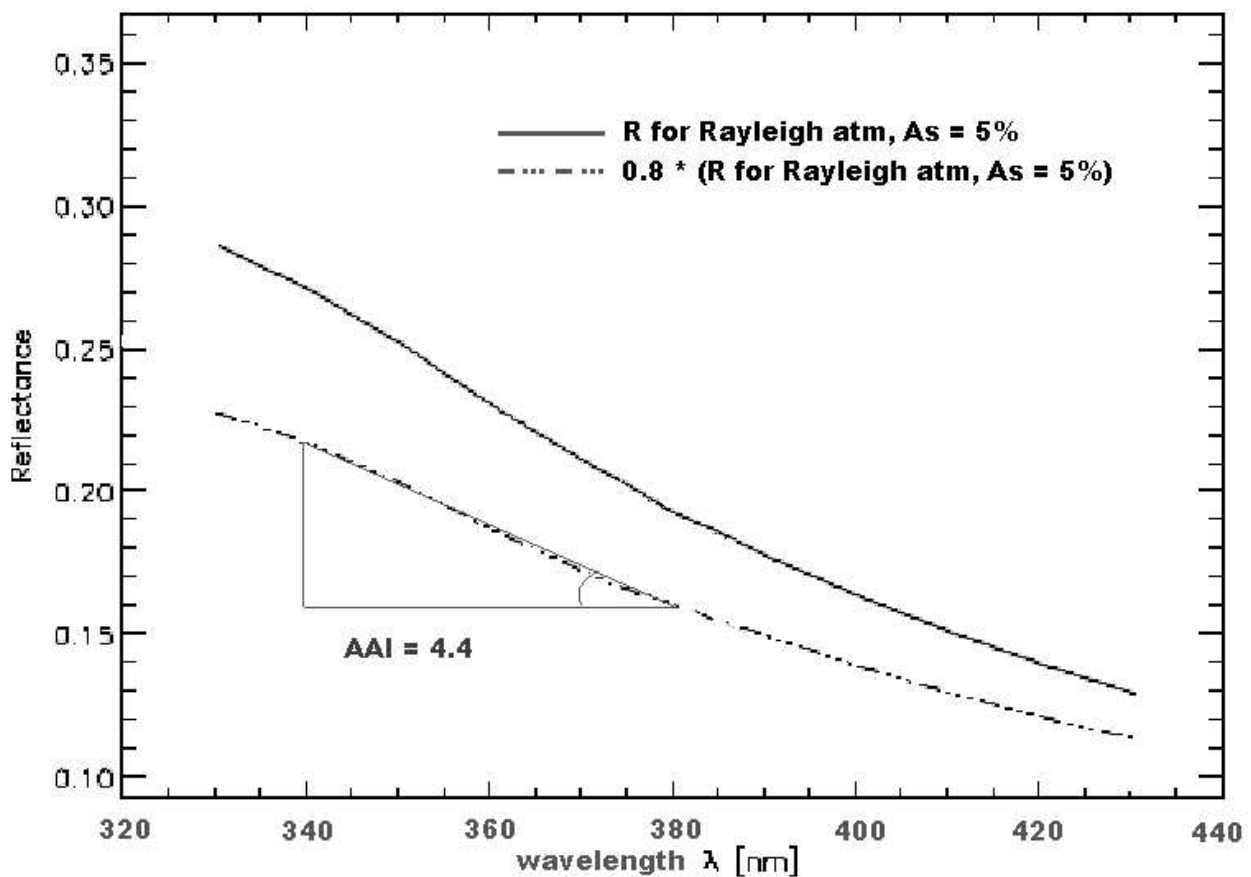


Fig. 4: Reflectance by a Rayleigh atmosphere, nadir view, solar zenith angle =  $30^\circ$ , surface albedo = 5% (solid line). Reducing the reflectance with 20% (dashed dotted line) reduces the slope between the signal at 340 nm and 380 nm. This introduces an artificial AAI of 4.4 in this case.

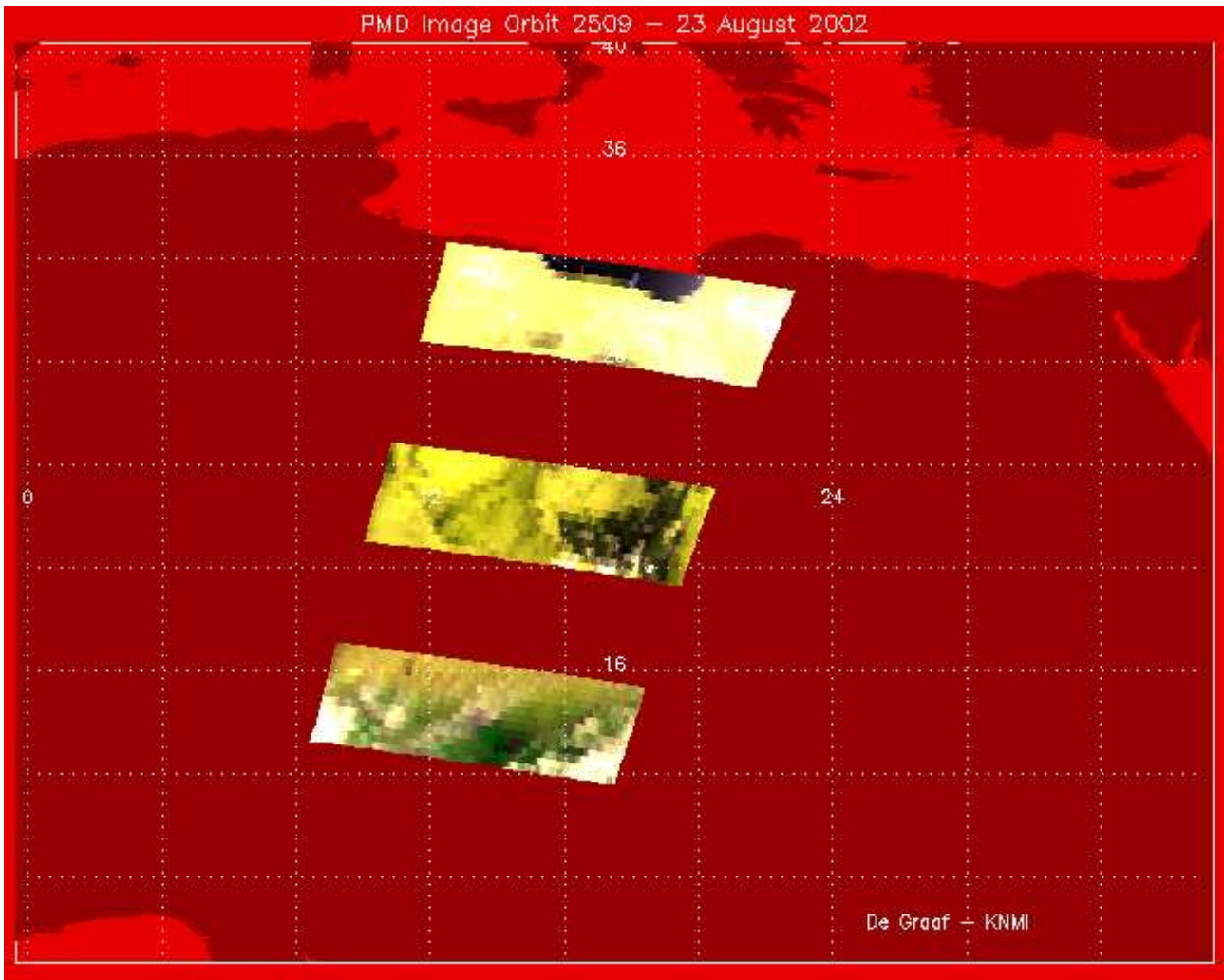
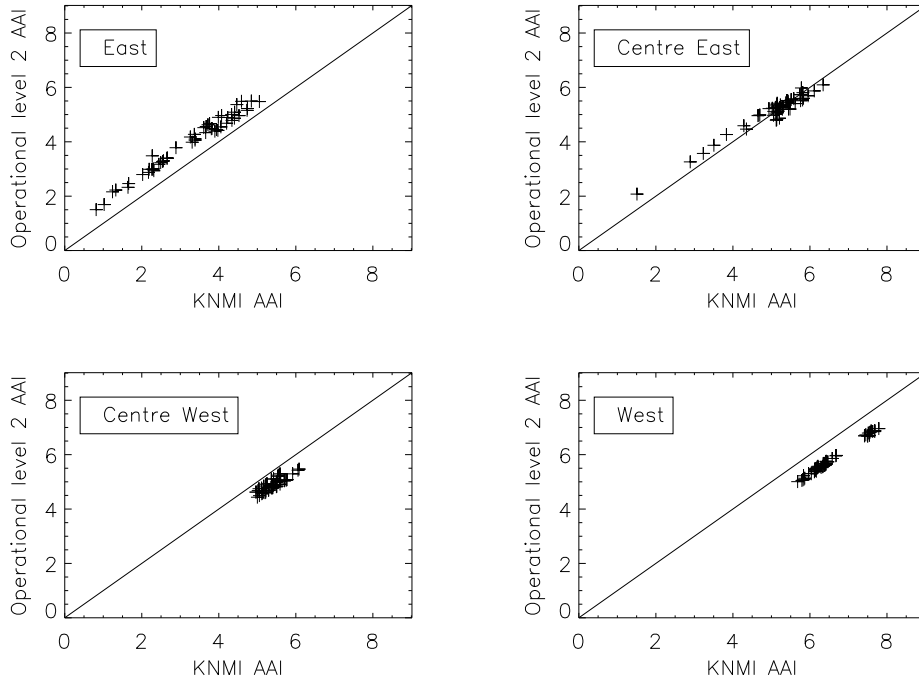


Fig. 5: Color image using PMD images of the Sahara region, orbit 2509 on 23 August 2002.

Fig. 2b also shows the light band in the extreme west pixels. This is probably caused by the problem of the reduced signal in these pixels as reported by several workers at the Envisat Geophysical Validation Workshop in December 2002. A reduced signal will increase the aerosol index, when the reduction is proportional to the original signal, as shown before in fig. 4. This problem could be due to an obstruction in the field of view of the instrument. It is unclear at the moment if this problem can be resolved.

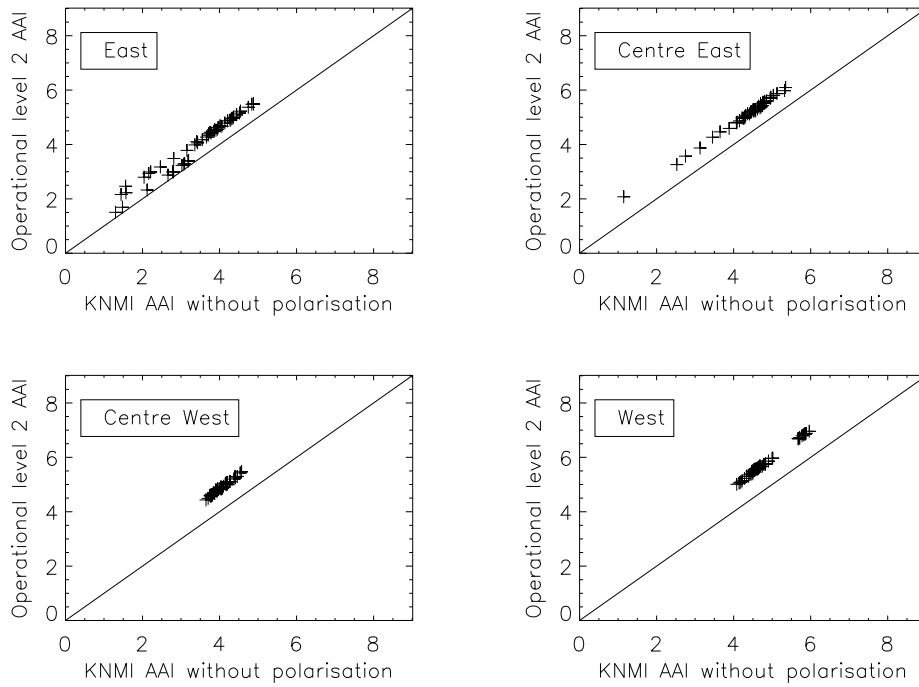
From fig. 3 it is clear that the operational level 2 product has lower amplitudes than the KNMI AAI. As both use the level 1 reflectances as input, the difference between the two AAIs must lie in the level 1 to 2 processing. In this case the difference is probably a result from the LUTs used. This means that the neglect of polarisation is probably the cause of the difference shown here. To investigate this the operational AAI and the KNMI AAI have been compared for each pixel. Five pixels are usually distinguished: an east pixel, a centre east pixel, a centre west pixel, a west pixel and a back scan pixel. The back scan pixel is not regarded here, as it is merely a necessary by-product of the scan mirror sweeping back to its starting position. The four other pixels each have different viewing angles and different polarisation properties. In fig. 6a the operational level 2 product is compared to the KNMI AAI for each pixel in state 12 separately. In the east pixels the values of the first are slightly higher than the level 1 AAIs, while in the west pixels the latter are higher. This is caused by the neglect of polarisation in the LUTs, which is consistently of reversed sign in east and west pixels. To show this fig. 6b shows the same AAI comparison, but now in the KNMI algorithm the LUTs have been replaced by LUTs in which polarisation has been neglected, as in the operational product. We now see there is still an off-set between

AAI Orbit 2509 state 12 ( 22°N, 15°E)



a

AAI Orbit 2509 state 12 ( 22°N, 15°E)



b

Fig. 6: a) Comparison of operational level 2 AAI and KNMI AAI of state 12, orbit 2509, per pixel. b) Same as a) but now the KNMI AAI algorithm uses LUTs in which polarisation has been neglected.

the operational product and the KNMI AAI. This must be caused by differences in the radiative transfer codes used or by differences in the parametrisation of the geometry. But the shift of higher operational AAIs at east pixels to lower operational AAIs at west pixels has vanished, which shows that this shift is probably due to polarisation effects in the LUTs.

## 7. CONCLUSIONS

Being dependent on the Earth's reflectances at two UV wavelengths only, the AAI can be well used for the verification of SCIAMACHY's level 1 UV reflectances. Doing so we clearly find all the problems of the level 1 products reported so far reflected in the AAI signal. The KNMI AAI algorithm, developed to account for polarisation, shows similar results as the operational level 2 product. This is because both algorithms use the level 1 reflectances as input, which is still subject to large errors. Comparing the two algorithms we do see polarisation-related differences of ten to twenty percent. So polarisation in the LUTs used in the level 1 to level 2 processing has a considerable influence on the calculation of the AAI, as was anticipated from sensitivity studies. It would be advisable to create new Look-Up Tables for SCIAMACHY's AAI, which take polarisation into account.

## 8. ACKNOWLEDGEMENTS

This work was sponsored by the Netherlands Agency for Aerospace Programmes (NIVR), project KN 11.201, "SCIAMACHY Core Validation of Aerosols".

## 9. REFERENCES

1. De Graaf, M. 2002, 'Sensitivity study of the residue method for the detection of aerosols from space-borne sensors.', Scientific Report WR-2002-03, Royal Netherlands Meteorological Institute (KNMI).
2. DLR, 'SCIAMACHY Level 1c to 2 Off-line Processing: Algorithm Theoretical Basis Document (ATBD)', Dec. 21, 2000.
3. Stammes, P. 2001, 'Spectral radiance modelling in the UV-visible range.' In: W. Smith and Y. Timofeyev (Eds), *IRS 2000: Current problems in atmospheric radiation*, pp. 385-288. A. Deepak Publishing, Hampton (VA).
4. Tilstra, L.G., M. de Graaf and P. Stammes. 2002. 'First verification of SCIAMACHY's polarisation measurements.', Envisat Calibration Review Proceedings, ESA, SP-520, Sept. 2002